On the accuracy of a logarithmic extrapolation of the wind speed measured by horizontal lidar scans

On the accuracy of a logarithmic extrapolation of the wind speed measured by horizontal lidar scans

F Theuer[1], M F van Dooren[1], L von Bremen[2] and M Kühn[1]

[1]ForWind, Institute of Physics, University of Oldenburg, Küpkersweg 70, 26129 Oldenburg, Germany
[2]DLR Institute of Networked Energy Systems, Carl-von-Ossietzky-Str. 15, 26129 Oldenburg, Germany

E-mail: frauke.theuer@uni-oldenburg.de

Abstract. Remote sensing-based wind power forecasts are nowadays being increasingly investigated. Long-range lidar scans are hereby often performed at low heights, causing the need for a wind speed extrapolation to hub height. In this work we analysed the accuracy of the stability corrected logarithmic wind profile and its sensitivity to atmospheric stability, wind speed and extrapolation height by means of a theoretical error estimation using error propagation. Emphasis was given to analyse the contributions of the profile's individual variables but also considering the measurement campaign framework. We further used lidar measurements at the offshore wind farm Global Tech I to support the theoretical analysis. The logarithmic profile was found to be able to describe profiles during most situations, however, decreasing wind speeds with height cannot be represented. Results showed that due to the nature of the stability correction term extrapolation errors are largest during very stable atmospheric conditions. Here, stability estimation errors were dominant. Under near neutral and neutral atmospheric conditions the wind speed error contributed most to the overall error. We conclude that extrapolation errors can mainly be reduced by optimising the estimation of atmospheric stability using accurate measurement devices. Furthermore, the precise horizontal alignment of the lidar device is important.

1. Introduction

Wind speed and power forecasts are gaining increasing importance due to the rising share of wind energy in our energy system. Skilful forecasts can be valuable tools to improve grid stability, to reduce curtailment costs and for electricity trading applications [1, 2, 3]. Recently, minute-scale forecasts based on long-range remote sensing measurements have been intensively investigated and show very promising results [4, 5, 6]. Here, inflow regions of the wind farm or wind turbine are typically measured by means of horizontal Plan Position Indicator (PPI) scans, allowing to retrieve wind field information with high temporal and spatial resolution. With the growing amount of offshore wind energy, especially compact scanning lidar devices become more suitable for that purpose, as they are comparably cheap, easy to set up and can be positioned on transition pieces of turbines, nacelles or platforms [7].

When aiming to forecast power, knowledge about the wind speed at hub height is crucial. As PPI lidar scans are typically performed at lower and in most cases varying measuring heights, due to misalignments and tilts of the devices [8], the need for skilful vertical wind speed extrapolation methodologies arises. A common way of extrapolation is the stability corrected logarithmic wind

profile [9]. However, while logarithmic profiles are based on physical considerations, i. e. the Monin-Obukhov similarity theory (MOST), they are also restricted by a number of assumptions, for example, the negligence of wind direction variations with height [10]. In addition to the physical restrictions of the profile, errors are introduced by misestimation of its individual parameters. As an inaccurate estimation of hub height wind speed can cause significant errors in power prediction, an assessment of the extrapolation accuracy is useful. Several studies comparing theoretically derived and measured profiles [9, 10] and analysing the impact of the profile's individual parameters, for example, temperature [11] and roughness length [12], on the error of vertical extrapolated wind speed have been performed. In our work, we want to focus on quantifying the contributions of the different parameters to the overall error. In our study also the discussion of errors introduced by the measurement set-up is of special importance.

This study aims to gain insight into the overall applicability of the logarithmic wind profile as well as to identify the most crucial error contributors in order to formulate suggestions for future measurement campaigns with the purpose of very short-term wind power forecasting. To do so we performed a sensitivity study of wind speed extrapolation errors with regard to i) atmospheric stability, ii) wind speed and iii) extrapolation height. The study is based on a theoretical error estimation of the stability corrected logarithmic wind profile as well as measurement data from a PPI lidar campaign at an offshore wind farm. Instead of horizontal scans, we analysed high elevation scans as a reference wind profile. Our work also includes an estimation of individual error contributions considering the set-up of the offshore lidar measurement campaign.

The results presented here are expected to be of interest for other areas of application as well, for example, wind farm control or wake tracking.

2. Methodology

This work is divided into a theoretical part, based on an error propagation of the logarithmic wind profile, and a practical part, based on PPI lidar measurements at the offshore wind farm Global Tech I (GT I). In the following, we will introduce the theoretical error estimation as well as the case study at GT I and its associated error values.

2.1. Theoretical error estimation

We analysed the accuracy of the stability-corrected logarithmic wind profile using the following equation:

$$u = \sqrt{\frac{z_0\, g}{\alpha_c}}\frac{1}{\kappa}\left(\ln\left(\frac{z}{z_0}\right) - \Psi\left(\frac{z}{L}\right)\right) \tag{1}$$

Here g is the gravitational acceleration, $\kappa = 0.4$ is the Von-Kármán constant, L describes the Obukhov length and z_0 is the roughness length. The Charnock parameter is set to $\alpha_c = 0.011$ [13]. To extrapolate wind speeds from the measuring height to hub height Equation (2) was used.

$$u_{\mathrm{hh}} = u_{\mathrm{m}}\frac{\ln(\frac{z_{\mathrm{hh}}}{z_0}) - \Psi(\frac{z_{\mathrm{hh}}}{L})}{\ln(\frac{z_{\mathrm{m}}}{z_0}) - \Psi(\frac{z_{\mathrm{m}}}{L})} \tag{2}$$

Here, z_{m} is the measurement height, z_{hh} is the hub height and u_{m} is the measured wind speed. The stability correction term is expressed as $\Psi\left(\frac{z}{L}\right)$ and defined as stated in Equation (3) following the definition of [14] with the parameters $\beta = 6$ and $\gamma = 19.3$ [15]. Indices of Ψ refer to the height z used to determine the correction term.

$$\Psi = \begin{cases} 2\ln\left(\frac{1+x}{2}\right) + \ln\left(\frac{1+x^2}{2}\right) - 2\arctan(x) + \frac{\pi}{2} & L < 0,\ \text{where } x = (1-\gamma\frac{z}{L})^{1/4} \\ -\beta\frac{z}{L} & L \geq 0 \end{cases} \tag{3}$$

Each of the parameters mentioned is associated with an error, contributing to the overall error of the estimated wind speed at hub height Δu_{hh}, which can be described as follows:

$$\Delta u_{\mathrm{hh}} = \left|\frac{\ln(\frac{z_{\mathrm{hh}}}{z_0}) - \Psi_{\mathrm{hh}}}{\ln(\frac{z_{\mathrm{m}}}{z_0}) - \Psi_{\mathrm{m}}}\right| \Delta u_{\mathrm{m}} + \left|\frac{u_{\mathrm{m}}(\ln(\frac{z_{\mathrm{hh}}}{z_0}) - \Psi_{\mathrm{hh}} + \Psi_{\mathrm{m}} - \ln(\frac{z_{\mathrm{m}}}{z_0}))}{z_0(\ln(\frac{z_{\mathrm{m}}}{z_0}) - \Psi_{\mathrm{m}})^2}\right| \Delta z_0 \tag{4}$$
$$+ \left|\frac{u_{\mathrm{m}}(\Psi_{\mathrm{hh}} - \ln(\frac{z_{\mathrm{hh}}}{z_0}))}{z_{\mathrm{m}}(\ln(\frac{z_{\mathrm{m}}}{z_0}) - \Psi_{\mathrm{m}})^2}\right| \Delta z_{\mathrm{m}} + \left|\frac{u_{\mathrm{m}}}{\Psi_{\mathrm{m}} - \ln(\frac{z_{\mathrm{m}}}{z_0})}\right| \Delta \Psi_{\mathrm{hh}} + \left|\frac{u_{\mathrm{m}}(\ln(\frac{z_{\mathrm{hh}}}{z_0}) - \Psi_{\mathrm{hh}})}{(\ln(\frac{z_{\mathrm{m}}}{z_0}) - \Psi_{\mathrm{m}})^2}\right| \Delta \Psi_{\mathrm{m}}$$

The error of the stability correction term $\Delta\Psi$ is summarised in Equation (5) and consists of the error in stability ΔL and the error in height Δz.

$$\Delta\Psi = \begin{cases} \left|\frac{4x^2}{x^3+x^2+x+1}\right| \Delta x & L < 0, \\ & \text{where } \Delta x = \left|-\frac{\gamma}{4L}\left(1-\gamma\frac{z}{L}\right)^{-3/4}\right| \Delta z + \left|\frac{\gamma z}{4L^2}\left(1-\gamma\frac{z}{L}\right)^{-3/4}\right| \Delta L \\ \left|-\beta\frac{1}{L}\right| \Delta z + \left|\beta\frac{z}{L^2}\right| \Delta L & L \geq 0 \end{cases} \tag{5}$$

In the course of this study, we assessed to what extent each of the components contributes to the overall error.

2.2. Case study at the offshore wind farm Global Tech I

In addition to the theoretical error estimation, we tested the extrapolation to hub height by means of Equation (2) using lidar measurements at the offshore wind farm GT I. GT I is positioned in the German North Sea and consists of 80 Adwen AD 5-116 5 MW turbines. The position and layout of the wind farm are depicted in Figure 1. PPI lidar scans were performed with an elevation of 13.57° from the free-stream wind turbine T2, marked in red in Figure 1 (b), thus measuring its inflow. Lidar measurements were conducted with measuring heights ranging from 36 m to 236 m, with azimuths between 134° and 313° and with a measurement time per scan of 44 s. For the purpose of extrapolation validation, we exemplary use high elevation scans instead of horizontal PPI scans for this analysis. Measured line-of-sight wind speeds were filtered using a carrier-to-noise ratio (CNR) threshold filter [5] and transformed to horizontal wind speeds by means of a Velocity-Azimuth Display (VAD) algorithm [16] individually for each range gate. During some periods extremely high variations of wind speed were observed, indicating faulty VAD fits. We used the wind speed's standard deviation within moving intervals as a measure to remove this low-quality data. A thrust dependent tilt of the lidar device observed during the measurement campaign was accounted for by means of an empirical correction function. The tilt's magnitude was hereby determined by applying a sea-surface-levelling procedure developed by [17]. Also, the Earth's curvature was considered during the calculation of the measuring height. Influences of the tide, which was found to vary approximately ±0.6 m, were neglected for simplicity. Measurements influenced by the induction zone were corrected [18] by means of an empirically derived axial induction factor. It was determined by fitting SCADA wind speed and power data to the wind turbine power curve. Hereby, we did not distinguish between different operating conditions of the turbine. Only situations for which the turbine is placed in free stream conditions, that is for wind inflow directions of 170° to 280°, are considered for this analysis. In total, a number of 2446 scans in the period between 16/10/2018 and 22/10/2018 were used.

Meteorological sensors as well as a buoy close to the lidar device measured pressure, humidity, air and water temperature and were used to estimate L according to [19]. z_0 was determined by

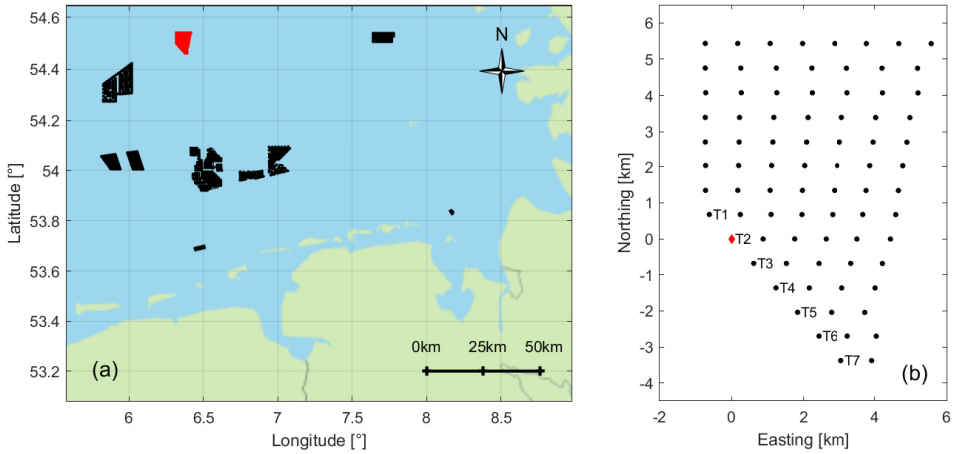

Figure 1. (a) Location of the wind farm Global Tech I in the German North Sea. GT I is shown in red, while other wind farms operational at the time of the lidar campaign are depicted in black. (b) Layout of GT I with turbines marked as black dots. The lidar is positioned on the transition piece of turbine T2, marked as ♦.

fitting lidar wind speed measurements at the closest range gate to Equation (1). Wind speeds were extrapolated from the lowest available height at 36.4 m to hub height at 92 m. Results were validated using lidar measurements at hub height. The quality of the extrapolation was assessed by means of the root-mean-squared error (rmse), the mean absolute error (mae) as well as the bias and distinguishing between atmospheric stability. Here, situations with $0\,\mathrm{m} < L < 1000\,\mathrm{m}$ were considered as stable, situations with $-1000\,\mathrm{m} < L < 0\,\mathrm{m}$ as unstable and all other cases as neutral. The analysed dataset consists of 924 stable, 1416 unstable and 106 neutral 44 s-mean cases. In a further step, we analysed the extrapolation accuracy dependent on wind speed and extrapolation height, again distinguishing between atmospheric stability.

For the theoretical analysis by means of Equation (4) a set of variables was defined considering the framework of the campaign. The roughness length was set to $z_0 = 0.0002\,\mathrm{m}$, a typical value for offshore conditions. As during the lidar campaign we determined z_0 by fitting to measurement data, we assumed its error to be relatively large and thus set it to $\Delta z_0 = 0.00002\,\mathrm{m}$. Line-of-sight wind speed errors of the lidar device are in the range of $0.2\,\mathrm{ms}^{-1}$ for small distances [20]. Additionally, we need to consider errors caused by the VAD fit, by spatial averaging along the beam direction and by limitations in pointing accuracy. We chose $\Delta u_\mathrm{m} = 0.5\,\mathrm{ms}^{-1}$ as a realistic estimate of an error associated with the mean lidar measured wind speed. Heights were set to $z_\mathrm{m} = 36\,\mathrm{m}$ and $z_\mathrm{hh} = 92\,\mathrm{m}$ in accordance with the measurement data. As lidar measurements were performed at small distances from the device, the error caused by the tilt of the device was comparably small. Δz_m was instead dominated by the influence of the tide and thus set to $\Delta z_\mathrm{m} = 0.6\,\mathrm{m}$. The stability error is dominated by temperature measurement errors. We did not investigate its impact further during this analysis, but kept ΔL constant at a value of $\Delta L = 10\,\mathrm{m}$.

3. Results

In the following we present the extrapolation error's dependency on i) atmospheric stability, ii) wind speed and iii) extrapolation height both theoretically and by means of the GT I data.

3.1. Stability dependency

Figure 2 (a) shows the overall error and its sub-components as described in Equation (4) varying with atmospheric stability. Here, all other variables are kept constant (see Figure 2), following

Table 1. Limits of the individual error components of Equation (4) for $L \to 0$ and $L \to \infty$ for both stable and unstable cases. Neutral refers to the neutral wind speed profile.

		u_{hh}	u_{m} comp.	z_0 comp.	z_{m} comp.	Ψ_{hh} comp.	Ψ_{m} comp.
$L \to \infty$	unstable	neutral	neutral	neutral	neutral	0	0
	stable	neutral	neutral	neutral	neutral	0	0
$L \to 0$	unstable	u_{m}	Δu_{m}	0	0	∞	∞
	stable	$\frac{z_{\mathrm{hh}}}{z_{\mathrm{m}}} u_{\mathrm{m}}$	$\frac{z_{\mathrm{hh}}}{z_{\mathrm{m}}} \Delta u_{\mathrm{m}}$	0	0	∞	∞

the error estimations from Section 2.2. We omitted the notion that errors of Obukhov length can result in a misclassification of stable situations as unstable ones and vice versa. Considering this would result in more severe extrapolation errors for cases $|\Delta L| > |L|$. Limits of the individual error components and the extrapolated wind speed u_{hh} are summarised in Table 1. For L with large absolute values, the wind speed error component contributes most to the overall error. For $L \to \infty$ Ψ and $\Delta\Psi$ approach 0, thus Δu_{hh} equals that of a neutral logarithmic wind profile, dominated by Δu_{m}.

With decreasing absolute values of L $\Delta\Psi_{\mathrm{hh}}$ and $\Delta\Psi_{\mathrm{m}}$ increase rapidly. For $L \to 0$ both Ψ and $\Delta\Psi$ approach infinity. As the stability correction errors increase more rapidly than the stability terms themselves, the error contributions of Ψ_{m} and Ψ_{hh} both approach infinity for $L \to 0$. Due to the definition of Ψ, as stated in Equation (3), it increases faster for stable than for unstable situations, explaining the larger errors for stable cases that can be observed in Figure 2 (a).

The error contributions of z_0 and z_{m} both approach zero for stable as well as unstable situations. The contribution of u_{m} approaches Δu_{m} for unstable situations as Ψ_{hh} and Ψ_{m} increase approximately at the same rate. For stable situations Ψ_{hh} grows more rapidly than Ψ_{m}, the u_{m} contribution here approaches $\frac{z_{\mathrm{hh}}}{z_{\mathrm{m}}} \Delta u_{\mathrm{m}}$. Thus for $L \to 0$ the logarithmic wind profile reaches its limits with $u_{\mathrm{hh}} = u_{\mathrm{m}}$ for unstable cases, that is a constant wind speed throughout height, and $u_{\mathrm{hh}} = u_{\mathrm{m}} \frac{z_{\mathrm{hh}}}{z_{\mathrm{m}}}$ for stable situations, that is a linearly increasing wind speed. More extreme wind speed profiles, for example decreasing wind speeds with height [21] or also very strongly increasing winds, cannot be described by Equation (1). The analysis of the VAD scans has shown that while the latter scenario did not occur, a decrease of wind speed with height could be observed in 8.8 % of the unstable, 1.9 % of the neutral and 19.3 % of the stable cases, which results in 12.4 % of all analysed cases. Møller et al. [21] have shown that kinks or local maxima of wind speed profiles occur quite commonly during both unstable and stable situations. During stable situations, a larger amount of reversed profiles can be observed, possibly related to low-level jets.

After theoretically assessing the stability dependency of the extrapolation error, we analysed the measurement data in regard to this. In Figure 2 (b) we compare the lidar wind speed at hub height with the lidar measurements extrapolated from the lowest measured height at 36.4 m to hub height at 92 m for unstable and neutral situations in blue, while in red stable situations are depicted. Whereas the overall agreement between measurements and extrapolated values was quite good for unstable and neutral cases with a rmse of $0.82\,\mathrm{ms}^{-1}$ and a mae of $0.57\,\mathrm{ms}^{-1}$, the extrapolation of stable cases showed very low quality with rmse $= 1.99\,\mathrm{ms}^{-1}$ and mae $= 1.77\,\mathrm{ms}^{-1}$. While during unstable and neutral situations the true value was being slightly underestimated with a bias of $-0.34\,\mathrm{ms}^{-1}$, the stable cases' bias was very low with $-0.03\,\mathrm{ms}^{-1}$. Considering Figure 2 (b) it becomes clear that both strong over- and underestimations of wind speed occurred, which cancelled out and thus yielded a very small bias. That means, in this case no systematic over- or underestimation of wind speed occurs. However, a small bias does

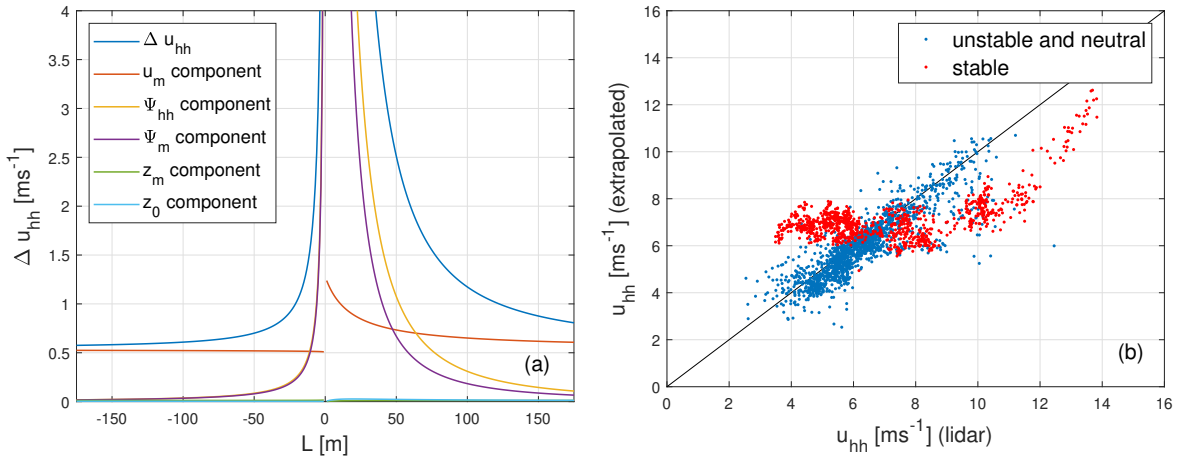

Figure 2. (a) Overall error Δu_{hh} and its sub-components following Equation (4) for varying atmospheric stability. All other variables were kept constant with $u_{\mathrm{m}} = 8\,\mathrm{ms}^{-1}$, $\Delta u_{\mathrm{m}} = 0.5\,\mathrm{ms}^{-1}$, $z_0 = 0.0002\,\mathrm{m}$, $\Delta z_0 = 0.00002\,\mathrm{m}$, $z_{\mathrm{m}} = 36\,\mathrm{m}$, $\Delta z_{\mathrm{m}} = 0.5\,\mathrm{m}$, $z_{\mathrm{hh}} = 92\,\mathrm{m}$ and $\Delta L = 10\,\mathrm{m}$. (b) Comparison of measured wind speeds at $z_{\mathrm{hh}} = 92\,\mathrm{m}$ and wind speeds extrapolated from $z_{\mathrm{m}} = 36.4\,\mathrm{m}$ for unstable and neutral (blue) as well as stable (red) situations.

not imply an accurate forecast. The results summarised here are in good agreement with those of the theoretical error estimation.

3.2. Wind speed dependency

Similar to the changes in stability, we analysed the impact of wind speed magnitude on the extrapolation error. Figure 3 (a) shows how Δu_{hh} and its sub-components behave with increasing values of u_{m}. The Obukhov length was set to $L = 150\,\mathrm{m}$ in this case, thus depicting a stable situation, all other variables were kept as stated in Figure 2. All sub-components except component u_{m} increase linearly with u_{m}, consequently also Δu_{hh} does. This effect is more distinct for very stable situations, as here the magnitude of especially the Ψ_{m} and Ψ_{hh} components is large. When analysing the lidar measurements, such a trend was not visible. Figure 3 (b) shows the mae's dependency on the wind speed at measuring height z_{m} distinguishing between atmospheric stability. Error bars indicate its standard deviation. We assume a dependency of the mae on wind speed is not visible here, as other influences, such as the varying stability throughout the measurements dominate. In accordance with the results of the previous section, errors for stable situations were generally higher than those for unstable cases.

3.3. Extrapolation height dependency

The extrapolation height $\Delta z = z_{\mathrm{hh}} - z_{\mathrm{m}}$ is defined by the initial height, i.e. the measuring height z_{m} and the final height, i.e. the hub height z_{hh}. Varying these heights significantly impacts the accuracy of the extrapolation. Figure 4 (a) depicts how the extrapolation height influences the individual error components. Here, the initial height was kept constant at $z_{\mathrm{m}} = 36\,\mathrm{m}$. All other variables were set as previously defined. L was set to 150 m. With larger extrapolation heights the error contributions of all sub-components and thus also the overall error Δu_{hh} increase.

To relate these results to the impact of atmospheric stability on the extrapolation accuracy we show the relationship between Δu_{hh} and L for the three cases $\Delta z = z_{\mathrm{hh}} - 36\,\mathrm{m}$, $\Delta z = z_{\mathrm{hh}} - 82\,\mathrm{m}$ and $\Delta z = 46\,\mathrm{m} - 36\,\mathrm{m}$ in Figure 4 (b). In good agreement with the previous results, extrapolation errors decrease when extrapolating across smaller distances for both stable as well as unstable

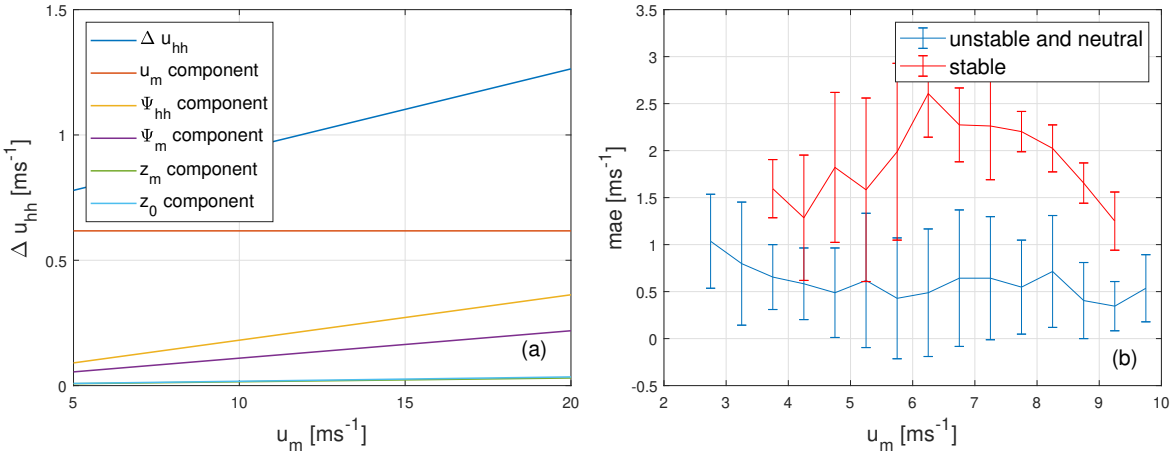

Figure 3. (a) Overall error Δu_{hh} and its sub-components following Equation (4) for varying wind speed. All other variables were kept constant as stated in Figure 2. (b) mae of the VAD extrapolation dependent on wind speed for unstable and neutral (blue) as well as stable (red) situations. Error bars indicate the mae's standard deviation.

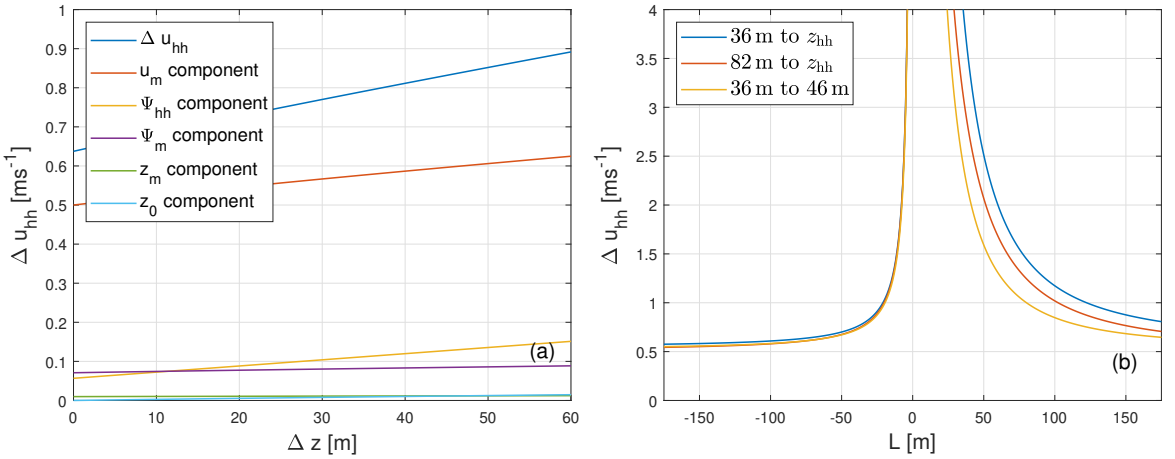

Figure 4. (a) Overall error Δu_{hh} and its sub-components following Equation (4) for varying extrapolation heights. The initial height z_{m} was kept constant at 36 m. All other variables were defined as stated in Figure 2. In (b) Δu_{hh} is shown for varying atmospheric stability and differing z_{m} and z_{hh}. All other variables were defined as stated in Figure 2

.

cases. Again, this effect is much more distinct during stable situations. As shown in Figure 4 (a) the change of extrapolation height mainly influences the error of the components u_{m} and Ψ_{hh}. For stable stratification, the contribution of these terms to the overall error is much larger than during unstable ones. Consequently, their reduction has a more significant impact.

Figure 4 (b) further shows the influence of the initial height z_{m} on the extrapolation error: Even though the extrapolation height Δz was the same for both $z_{\mathrm{hh}} - 82\,\mathrm{m}$ (red) and $46\,\mathrm{m} - 36\,\mathrm{m}$ (yellow), the error reduction is more distinct in the lower region of the wind speed profile. For lower values of z_{m} especially $\Delta\Psi_{\mathrm{m}}$ and $\Delta\Psi_{\mathrm{hh}}$ are reduced as here z contributes linearly. This causes larger errors in higher altitudes despite the steeper increase of wind speed in lower heights.

We also performed a sensitivity analysis of the extrapolation height by means of the lidar

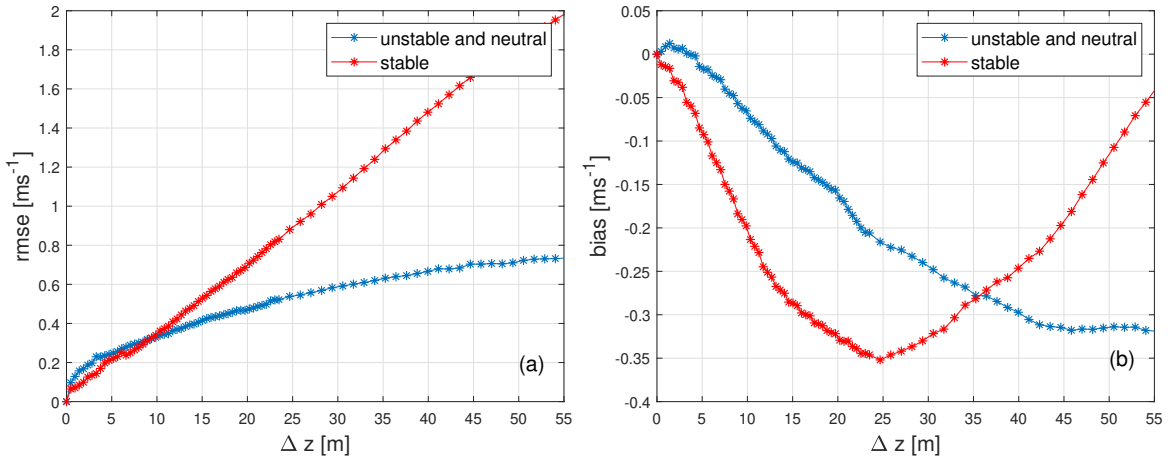

Figure 5. Dependency of (a) rmse and (b) bias of wind speed extrapolation on the extrapolation height with fixed initial height $z_{\mathrm{m}} = 36.4\,\mathrm{m}$ for unstable and neutral (blue) as well as stable (red) situations.

measurements. The initial height was chosen as the minimal available measurement height of approximately 36.4 m. A wind speed extrapolation with increasing extrapolation heights Δz and consequently varying final heights z_{hh} was performed and evaluated using the lidar wind speed measurements. Rmse and bias were calculated distinguishing between stable and the combination of neutral and unstable atmospheric conditions. The results are depicted in Figure 5. For stable cases, the rmse decreases linearly from a maximum value of about $2\,\mathrm{ms}^{-1}$ at an extrapolation height of 55 m to a value of $0\,\mathrm{ms}^{-1}$. For neutral and unstable cases, the rmse decreases logarithmically, but at a much smaller rate. Here, rmse values were much lower with $0.7\,\mathrm{ms}^{-1}$ at 55 m but only decrease to $0.25\,\mathrm{ms}^{-1}$ at 5 m. For extrapolation heights below 5 m the rmse then further decreases until it also reaches $0\,\mathrm{ms}^{-1}$. These results clearly illustrate, in good agreement with the findings of the theoretical error estimation, that reduced extrapolation heights diminish extrapolation errors and have a much more distinct impact during stable situations as compared to neutral and unstable ones.

In Figure 5 (b) the bias of unstable and neutral cases strongly improves with decreasing Δz. The bias is almost constant with $-0.32\,\mathrm{ms}^{-1}$ down to $\Delta z = 43\,\mathrm{m}$ before it decreases linearly to reach a value of $0\,\mathrm{ms}^{-1}$ at $\Delta z = 0\,\mathrm{m}$. For stable cases the bias worsens from $-0.05\,\mathrm{ms}^{-1}$ to $-0.35\,\mathrm{ms}^{-1}$ from extrapolation heights of 55 m to 25 m. It then strongly improves until reaching $0\,\mathrm{ms}^{-1}$ at $\Delta z = 0\,\mathrm{m}$. Both graphs indicate a tendency to underestimate wind speed. A more detailed data analysis has shown that for unstable and neutral situations the wind speed extrapolation according to the logarithmic profile is too small compared to the true wind speed variation with height, resulting in an underestimation of wind speed. For stable cases, this also holds when extrapolating to heights up to approximately 90 m. For higher altitudes, the effect reverses, in those cases the extrapolation is too strong. As we are only considering altitudes up to hub height this overestimation of wind speed is not visible in Figure 5 (b). We will discuss this in more detail in Section 4. As mentioned earlier, a small bias is not necessarily an indication for an accurate forecast.

4. Discussion

Our analysis aimed to assess the error associated with a stability-corrected logarithmic wind profile for wind speed extrapolation to hub height, based on horizontal lidar scans measured during an offshore campaign. For that purpose, we performed a sensitivity study and analysed

high elevation PPI lidar scans as a reference wind profile. Generally, the logarithmic profile was found suitable to describe the wind speed development with height for most situations. However, profiles showing abnormalities such as kinks or reversed profiles cannot be described using a logarithmic profile. Such profiles are not uncommon, especially during stable situations, as confirmed by recent studies [21]. As wind speeds are almost uniform with height during unstable situations, the observed abnormalities do not cause very significant deviations between extrapolated and true profiles. During stable situations, however, wind speeds are described as strongly increasing with height. Reversed profiles, for example, observed during low-level jets, can thus not be well represented by logarithmic profiles.

A sensitivity study has shown that, especially during stable atmospheric stratification, extrapolation errors are large due to the nature of the stability correction term. Furthermore, the wind speed and the extrapolation height impact the error's magnitude. In both cases, effects are particularly large during very stable situations. Although we are not able to impact atmospheric conditions such as stability or wind speed to reduce extrapolation errors, we can improve the accuracy of determining these parameters. The contributions of u_{m} and Ψ to the overall error are largest. While the reduction of wind speed errors, for example by improving wind speed reconstruction methodologies, is not trivial, stability errors can be diminished more easily. Here, the error mainly consists of temperature, pressure and humidity estimation errors that can have large impacts on the determined value of L. For example in [11] it is shown that small errors in temperature estimation already result in large errors in extrapolated wind speed. The temperature error's impact on the stability misestimation was hereby found to be very distinct, especially during very stable situations and for low wind speeds. A crucial part of improving wind speed extrapolation is thus the installation of reliable and accurate meteorological sensors that allow for a precise estimation of a stability parameter.

Further extrapolation uncertainty is introduced by the measuring height. While one can easily account for the Earth's curvature, height variations caused by the tide and a tilt of the lidar device are more difficult to consider. The lidar alignment is crucial for long-range measurements as differences in measuring height caused by an inclination of the device increase with distance. As an example, an elevation error of 0.1° causes a height difference of 8.7 m over a measuring distance of 5 km. While these contributions of z_{m} are rather small compared to those of wind speed and stability, especially during stable situations, they can significantly contribute to the overall error. Therefore, lidar devices should be carefully aligned and their orientation has to be thoroughly and regularly checked in order to be able to correct for any misalignments.

Comparing the results of the theoretical error estimation and the case study we find them generally to be in good agreement. We need to keep in mind, though, that the logarithmic profile is considered to be an optimal representation of true profiles during the theoretical estimation. The case study, on the other hand, also includes errors caused by the inapplicability of the profile itself. Especially during very stable situations, the logarithmic profile is not applicable as the surface layer, in which approximations based on MOST are considered valid, is much lower than the extrapolation domain [12]. Several studies have shown that logarithmic profiles tend to overestimate wind speed in larger heights during stable conditions due to decreasing wind speeds with height [21, 9]. In Figure 5 (b) we observed an improving bias at extrapolation heights from 25 m to 55 m. This can thus be interpreted as the region where an increased number of decreasing wind speeds with respect to wind speeds at initial height is considered, starting to counterbalance the underestimation of wind speed observed at lower altitudes. Consequently, the extrapolation height of 25 m and final height of 61 m can be interpreted as the height at which these decreases first start to occur. During unstable situations, on the other hand, logarithmic profiles present a good approximation of true wind speed profiles. Summarising, the large errors

observed during stable situations consist of uncertainties in the profile itself as well as those introduced by errors of individual parameters.

5. Conclusion

In this work we analysed the accuracy of a stability corrected logarithmic wind profile for wind speed extrapolation in the scope of very short-term power forecasts based on long-range scanning lidar data. A theoretical error estimation was performed and disclosed that large errors mainly occur under stable atmospheric conditions due to the definition of the stability correction term. Besides stability, also wind speed errors contribute strongly to the overall extrapolation error. We further showed that uncertainties can be reduced by decreasing the extrapolation height and are also increasing with wind speed. Results of the theoretical analysis were confirmed by the investigation of PPI lidar measurements performed at the offshore wind farm GT I. In order to reduce extrapolation errors in the proposed measurement framework, the authors suggest improving stability estimation and lidar alignment. Furthermore, the analysis revealed that logarithmic profiles are less applicable during stable situations, due to the occurrence of reserved profiles or kinks. In future work, the error sensitivity of further wind profiles should be investigated.

Acknowledgments

The lidar measurements and parts of the work were performed within the research project "OWP Control" (FKZ 0324131A) funded by the German Federal Ministry for Economic Affairs and Energy on the basis of a decision by the German Bundestag. We acknowledge the wind farm operator Global Tech I Offshore Wind GmbH for providing SCADA data and thank them for supporting our work. We further acknowledge the German Federal Environmental Foundation (DBU) as this project received funding within the scope of their PhD scholarship programme.

References

[1] Liang Z, Liang J, Wang C, Dong X, and Miao X 2016 *Energy Conversion and Management* **119** 215–26
[2] Dowell J and Pinson P 2016 *IEEE Transactions on Smart Grid* **7** 763–70
[3] Sweeney C, Bessa R J, Browell J, Pinson P 2019 *WIREs Energy Environ.* **9** 365
[4] Würth I, Ellinghaus S, Wigger M, Niemeier M J, Clifton A and Cheng P W 2018 *J. Phys.: Conf. Series* **1102** 012013
[5] Valldecabres L, Peña A, Courtney M, von Bremen L, and Kühn M 2018 *Wind Energ. Sci.* **3** 313–27
[6] Valldecabres L, Nygaard N, Vera-Tudela L, von Bremen L, and Kühn M 2018 *Remote Sens.* **10** 1701
[7] Würth, Valldecabres L, Simon E, Möhrlen C, Uzunoğlu B, Gilbert C, Giebel G, Schlipf D and Kaifel A 2019 *Energies* **12** 712
[8] Theuer F, Valldecabres L, von Bremen L and Kühn M 2019 *Wind Energy Science Conf. (Cork, Ireland)*
[9] Peña A, Gryning S-E and Hasager C B 2008 *Bound.-Lay. Meteorol.* **129** 479–95
[10] Optis M, Monahan A and Bosveld F C 2014 *Bound.-Lay. Meteorol.* **153** 497–514
[11] Saint-Drenan Y-M, Hagemann S, Lange B, Tambke J 2009 *European Wind Energy Conf. and Exhibition (Marseille, France)* pp 1-5
[12] Kelly M and Jørgensen H E 2017 *Wind Energ. Sci.* **2** 189-209
[13] Smith S D 1980 *J. of Phys. Oceanogr.* **10** 709–26
[14] Dyer A J 1974 *Bound.-Lay. Meteorol.* **7** 363–72
[15] Högström U 1988 *Bound.-Lay. Meteorol.* **42** 55–78
[16] Werner C 2005 *Lidar* ed K Weitkamp (New York: Springer New York) chapter 12 pp 325–54
[17] Rott A, Schneemann J, Trabucchi D, Trujillo J and Kühn 2017 *NAWEA WindTech (Colorado, USA)*
[18] Medici D, Ivanell S, Dahlberg J-Å and Alfredsson P H 2011 *Wind Energ.* **14** 691–97
[19] Sanz Rodrigo J, Cantero E, García B, Borbón F, Irigoyen U, Lozano S, Fernandes P M and Chávez R A 2019 *J. Phys.: Conf. Series* **625** 012044
[20] van Dooren M F, Trabucchi D and Kühn M 2016 *Remote Sensing* **8** 809
[21] Møller M, Domagalski P and Sætran L R 2020 *Wind Energ. Sci.* **5** 391-411